Gramicidin Channels Are Internally Gated

Tyson L. Jones,[†] Riqiang Fu,[‡] Frederick Nielson,[†] Timothy A. Cross,[‡] and David D. Busath[†*]
[†]Department of Physiology and Developmental Biology, Brigham Young University, Provo, Utah; and [‡]National High Magnetic Field Laboratory, Florida State University, Tallahassee, Florida

ABSTRACT Gramicidin channels are archetypal molecular subjects for solid-state NMR studies and investigations of single-channel or cation conductance. Until now, the transitions between on and off conductance states have been thought, based on multichannel studies, to represent monomer ↔ dimer reactions. Here we use a single-molecule deposition method (vesicle fusion to a planar bilayer) to show that gramicidin dimer channels do not normally dissociate when conductance terminates. Furthermore, the observation of two ^{13}C peaks in solid-state NMR indicates very stable dichotomous conformations for both the first and second peptide bonds in the monomers, and a two-dimensional chemical exchange spectrum with a 12-s mixing time demonstrates that the Val_1 carbonyl conformations exchange slowly, with lifetimes of several seconds. It is proposed that gramicidin channels are gated by small conformational changes in the channel near the permeation pathway. These studies demonstrate how regulation of conformations governing closed ↔ open transitions may be achieved and studied at the molecular level.

INTRODUCTION

As a model for ion conductance, gramicidin A (gA) has proved to be valuable for understanding cation binding, dehydration, and selectivity (1–5). Here, we suggest that it is also an excellent model for understanding the mechanisms by which channels open and close. The gA head-to-head dimer structure is well established for the conducting state (6,7) and has been characterized to very high resolution in a liquid crystalline lipid bilayer environment through the use of solid-state NMR (ssNMR) (8,9). For many reasons, monomer association and dissociation have been taken to be responsible for single-channel on and off transitions, respectively (10). These include the statistical distribution of channel levels (11), the nature of the dimer junction (six hydrogen bonds (12)), the long lifetimes of covalently-linked dimers (13), the quadratic dependence of channel activity on membrane peptide density (14), the similarity between membrane conductance perturbation relaxation time and single-channel gating rate constants (15–17), and the apparent success of the hypothesis in explaining heterodimer formation (15). But there is no direct evidence for this view. Although preliminary single-molecule fluorescence studies (16) suggested that channels begin to conduct only after dimerization occurs, and that the lifetime of fluorescence resonance energy transfer spots on average is similar to the average channel lifetime (16), it was subsequently shown that fluorescence resonance energy transfer intensity and monomer colocalization persist during channel off periods for single-channel patches (17). In other words, dimers do not dissociate when the ion channel closes.

It is also noteworthy that ssNMR results show that gA monomers do not float in leaflets, coiled and ready to dimerize, but instead are largely disordered on the surface (18). This contradicts the earlier, less specific in-plane x-ray scattering evidence (19) and suggests that dimerization must usually occur before membrane formation.

In thin bilayers, the gA dimer interface is stabilized by six hydrogen bonds at the very center of the lipid bilayer, and although the exact strength of such hydrogen bonds can be debated (20–23), it is reasonably believed that breaking all of the junctional hydrogen bonds in the low dielectric membrane interior would be a significant energetic challenge. Thus, the mechanism of channel opening and closure is currently under debate.

Here, we use a direct method to evaluate this issue. By fusing gA-doped vesicles to a planar lipid bilayer with the Woodbury nystatin technique (24), we can track the lifetime of individually deposited dimers. Because only a few molecules are delivered to the membrane, as opposed to the thousands of monomers typically present in the bilayer of previous studies, dimer dissociation can be expected to be terminal since no alternative partners are likely to be encountered by diffusion on the timescale of the experiment. The vesicle fusion results contradict the monomerization model for the termination of gA single-channel conductance, and suggest instead that there is an internal gating mechanism in gA.

In addition, we report ssNMR results from liquid crystalline lipid bilayer preparations indicating a peptide backbone conformational oscillation on a timescale similar to that observed for the channel gating process, which is a good candidate for the internal gate.

These findings facilitate the interpretation of ongoing gA electrophysiology studies (25) and are consistent with the suggestion that local conformational changes may underlie the open-close transition process for other protein ion channels, such as potassium (26) and sodium (27) channels.

Submitted June 3, 2009, and accepted for publication November 12, 2009.

*Correspondence: david_busath@byu.edu

Editor: Benoit Roux.

0006-3495/10/04/1486/8 $2.00

doi: 10.1016/j.bpj.2009.11.055

MATERIALS AND METHODS

Planar bilayer studies

Single-channel currents were obtained using a painted planar lipid bilayer composed of a mixture of phosphatidylethanolamine (PE) and phosphatidylcholine (PC), both from bovine brain or both with 1-palmitoyl, 2-oleoyl (PO; Avanti Polar Lipids, Alabaster, AL) tails as noted, in a molar ratio of 7:3, dispersed in *n*-decane (20–30 mg lipid/mL *n*-decane).

The liposome solution consisted of 10 ng gA, 50 μg nystatin, and 4.3 mg brain PE, 2.2 mg brain PC, 2.3 mg brain phosphatidyl serine (PS; or similar masses of PO lipids), and 1.2 mg ergosterol (Sigma-Aldrich, St. Louis, MO) per milliliter of 150 mM KCl, 8 mM HEPES, pH 7.2. We refer to this mixture according to its approximate lipid molar composition: 2:1:1:1. For tests of the raft confinement hypothesis, vesicles were comprised of 10 ng gA, 7 mg brain PE, and 3 mg brain PC (no ergosterol) per milliliter of the same electrolyte. Ergosterol was stored in the freezer for up to 6 months as a stock solution in chloroform (10 mg/mL). Methanolic nystatin (Sigma-Aldrich) stock solutions were prepared by dissolving 2.5 mg/mL in high-performance liquid chromatography-grade methanol. The methanol was kept dry (free of water) during storage to prevent nystatin from precipitating out of solution (24). Mild bath sonication was used to disperse the nystatin in methanol. Stock solutions of gA were prepared by dissolving 0.67×10^{-3} mg gA per milliliter of methanol (also dry). To prepare the vesicles, the lipid in chloroform and peptide in methanol were mixed and then evaporated with nitrogen gas to form a thin film. Then, electrolyte was added and the mixture was vortexed for 5 min and sonicated in a water bath sonicator (at 22°C) for 2 min. The mixture was cloudy after vortexing and became translucent after sonication. After incubation at 3°C for 0–14 days, vesicles were returned to room temperature, vortexed and/or sonicated, and then measured by dynamic light scattering (90Plus particle size analyzer; Brookhaven Instruments, Holtsville, NY) to be 200–250 nm in diameter, with a secondary peak at >600 nm. Channel activity was independent of the incubation period, suggesting that monomer-dimer equilibration was achieved during vesicle formation.

Lipid bilayers were formed by painting the 7:3 PE-PC in *n*-decane across the aperture (200 μm in diameter) in a polystyrene cup (Warner Instruments, Hamden, CT). The bilayer was painted in 150 mM KCl, 8 mM HEPES (both from Sigma-Aldrich), pH 7.2, in filtered, distilled water. $[KCl]_{cis}$ was raised to 860 mM by exchange with appropriate aliquots of 3 M KCl. A potential of −100 mV (*trans* relative to *cis*) was applied by means of Ag-AgCl electrodes placed directly in the *cis* and *trans* chambers. After correction for chloride potentials at the electrodes (taking activity coefficients into account), this corresponds to a membrane potential of −140 mV.

After an osmotic gradient was established and the membrane was judged from capacitance and baseline noise to be fully thinned, 10 μL of nystatin-ergosterol vesicle suspension were added to the *cis* chamber, which contained 1 mL, while stirring. After the liposome suspension was injected into the *cis* chamber, it thus contained 0.1 ng gA and 0.1 mg lipid. Fusion was initiated spontaneously. Typically, within 5–10 min of stirring after vesicle addition, vesicle fusions were observed, as signaled by sudden spikes in conductance due to nystatin channels, followed by decay back to the baseline conductance within ~1 min. This was thought to be due to dissipation of ergosterol, which is required for nystatin conductance, from the fusion site (24).

After one or two fusion events occurred, stirring was stopped, which essentially terminated vesicle fusion events. In some experiments, new fusions were blocked by increasing *trans* [KCl] to eliminate the osmotic gradient, with similar results. We were able to increase membrane conductance by reinitiating stirring, but this became increasingly less effective as the experiment progressed. We note that small vesicles may not cause measurable nystatin spikes, but because of the low density of gA in such liposomes, they should not contribute appreciably to gA delivery. All experiments were performed at temperatures between 22°C and 24°C.

Membrane currents were measured using a Warner BC-525C bilayer clamp amplifier (Warner Instruments). The amplifier gain was 100 mV/pA, except where lower gains were needed for multichannel experiments. Data were low-pass filtered at 100 Hz and collected continuously, at 300 samples/s, until membrane breakdown occurred, typically 30–90 min after bilayer formation. Data were collected on a PC computer with a PCI-12 data acquisition board (National Instruments, Austin, TX) and IGOR Pro (v. 3.01; Wave Metrics, Lake Oswego, OR). Current transitions reflecting channel openings and closings were detected and analyzed with the computer programs TAC and TACfit (v. 2.5; Skalar Instruments, Seattle, WA). To facilitate analysis, digital filtering was applied, usually with a cutoff of 30 Hz.

Control experiments with vesicles of similar composition, but without nystatin or ergosterol, yielded similar gA channel behavior, but with no nystatin current spikes. If the membrane was disrupted at any time during this preparation or the subsequent observation, the experiment was terminated. For activity studies, gramicidin density was increased from 10 to 100 or 1000 ng gA/10 mg lipid/mL buffer.

To test whether monomers could exchange partners after vesicle fusion, a PO 7:3/decane bilayer was painted, and methanolic gramicidin M (gM), the analog of gA with Trp-9, 11, 13, and 15 each replaced by Phe, was added to the *trans* chamber to a final concentration of 0.5 ng gM/1 mL solution. Once gM channels were observed, an osmotic gradient was introduced, and gA-containing PO 2:1:1:1 vesicles were added under stirring to the *cis* chamber to the usual final concentration of 0.1 ng gA/0.1 mg lipid/1 mL electrolyte solution until fusion spikes were observed. In each of three cases, experiments lasted more than 1 h after protein addition. Control experiments with gM and gA comingled (1:1) in the vesicles ($N = 3$) were used to identify conductance histogram peak positions for the two homodimers and two heterodimers under concentration gradient conditions.

NMR studies

^{13}C magic angle spinning (MAS) spectra of $^{13}C_1$-Val_1, ^{15}N-Ala_5 gA were obtained in unoriented, hydrated dimyristoylphosphatidylcholine (DMPC) bilayers with a molar peptide/lipid ratio of 1:8, with or without 2.4 M KCl in the aqueous phase (1). gA was synthesized by solid-phase peptide synthesis using 9-fluorenymethoxy-carbonyl chemistry on an Applied Biosystems (Foster City, CA) model 430A peptide synthesizer. The blocking chemistry of isotopically labeled amino acids was performed in our laboratory. After synthesis and cleavage, the peptides were characterized and purified, as detailed previously (28,29).

Unoriented samples for ssNMR were prepared by codissolving gA and DMPC in a 1:8 molar ratio in 95/5 (v/v) benzene/ethanol solution. After lyophilization, the white powder was hydrated by adding 50% high-performance liquid chromatography-grade water (by total sample dry weight). The K^+ loaded sample was prepared by hydration with a 2.4 M KCl solution, which should produce double K^+ occupancy in the dimer (30). The tubes were then sealed and incubated at 45°C for a minimum of 2 weeks until the samples became uniformly hydrated. The samples were then transferred into 4 mm ZrO NMR rotors with Vespel sealing caps for NMR measurements.

All high-resolution ^{13}C NMR measurements were performed on a Bruker DMX-600 NMR spectrometer ($B_0 = 14.1$ T) equipped with a Bruker cross-polarization MAS (CPMAS) double-resonance probe with 4 mm rotors and with Larmor frequencies of 150 MHz for ^{13}C and 600 MHz for ^{1}H. A standard chemical exchange pulse sequence (31) with CP was used to record the two-dimensional (2D) ^{13}C chemical exchange spectrum. All spectra were recorded at 320 K (above the gel-to-liquid crystalline phase transition temperature of the lipids) using CP (5 μs 90° pulse length and 700 μs contact time) and a sample spinning rate of 2 kHz. A recycle delay of 4 s was used, and the proton decoupling ($B_1 = 62$ kHz) was applied throughout the evolution and observation of the ^{13}C magnetization.

RESULTS

In the confines of a vesicle membrane, gA monomers are likely to be dimerized (14). Therefore, under the traditional hypothesis, we expected the fusion of a single vesicle to

deliver a few dimers into the bilayer, which should initially be open and then shut off upon dimer dissociation and never return. Instead, channel conductance events usually occurred within a brief period after fusion events and then recurred continuously for the duration of the experiment. This is illustrated in Fig. 1, *A* and *B*, where a few vesicles fused to the planar bilayer. In the first expanded box (Fig. 1 *B*, *left*), six characteristic nystatin current spikes occurred due to the fusion of vesicles containing preformed nystatin channels (32). These multichannel current spikes terminate rapidly as the channel-stabilizing ergosterol diffuses into the ergosterol-free painted bilayer.

Here the brain 2:1:1:1 vesicles delivered approximately five active dimers (the maximum number of simultaneously conducting pores; Fig. 1 *B*, *right*), which opened and closed repetitively for the lifetime of the brain 7:3 bilayer, 54 min. If monomerization occurred, the likelihood of recombination with the same or another monomer in the 200-μm bilayer would be negligible. Because the nystatin channels are known to reflect the timescale of ergosterol dissipation, i.e., several seconds (32), it further appears that the gA channels are not merely confined to vesicle-derived ergosterol-rich lipid domains. This result was duplicated in a second experiment of similar length.

To rule out the possibility that the vesicles merely formed long-lasting domains in the bilayer due to a difference in their lipid composition, we repeated the experiment with vesicles composed of the same lipid as the bilayer, i.e., brain 7:3. In 27 experiments that were similar to the two mentioned above in vesicle fusion and in duration (40–60 min), yielding maximum stacking levels (parallel conductance events) of one to eight channels, the same persistent channel activity was observed after cessation of vesicle fusion. In three of these experiments where no stacking was observed, the average channel lifetime, τ, was 4.8 s and the apparent open probability, P_o, averaged 0.027. Because of the long closed-state periods, the bilayers were not sufficiently long-lived to rule out the presence of multiple dimers in the bilayer. A membrane lasting $6\tau/P_o^2$ (>9 h) without stacking would be needed to establish this fact at the 95% confidence level (33). Nevertheless, the average lifetime of 4.8 s is trustworthy, and the value of P_o can be taken as an upper limit. Given the rapid dissipation of the nystatin signal, which depends on intermixing of vesicle nystatin and ergosterol molecules with the nystatin- and ergosterol-free planar bilayer (24) and the lipid-like diffusion coefficient of gA fluorescence signals (17), it is clear that within a minute or so of deposition, the gA dimer channel is surrounded by and responding to the bulk lipid environment, i.e., 7:3 brain PE-PC in decane.

To demonstrate that the channels delivered by vesicles to the bilayer cannot switch docking partners, we fused vesicles containing gA to bilayers preloaded with gM channels. In three separate experiments (totaling 391 conductance events), only rare heterodimers (4% ± 3%) were observed over the course of 60–90 min after vesicle fusion occurred (see Fig. 1 *C* for an example). In three separate experiments, gA and gM (1:1) were premixed in the vesicles and fused to a bilayer. Each time, four distinct peaks were observed in the histogram with a large fraction of heterodimers (38% ± 22%, from a total of 954 conductance events), with an expectation of 50% under the assumption of equivalent dimerization energetics (34). The experiments represented by Fig. 1 *C* show that the majority of gA molecules in the vesicles stay bound together in homodimers throughout fusion, and that the homodimers only rarely dissociate after vesicle fusion to partner with preexisting gM monomers in the bilayer during the experimental time course.

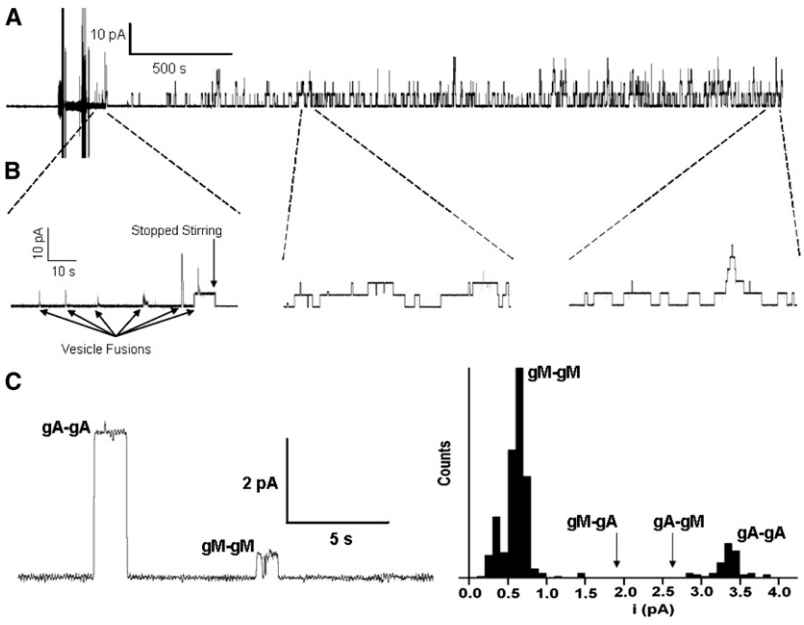

FIGURE 1 Planar-bilayer current resulting from fusion of gA-doped vesicles. (*A*) Zoomed-out view of an entire representative experiment. Brain 2:1:1:1 was used for vesicles, and brain 7:3 (in *n*-decane) was used to paint the bilayer. Scale: $y = 10$ pA, $x = 500$ s. Note two injection artifacts and stirring noise before the first excerpt. $V_m = -200$ mV. (*B*) Magnified excerpts showing persistent gA channel activity. Scale: $y = 10$ pA $x = 10$ s. Note the six nystatin current spikes representing fusion events during the first excerpt only, and the appearance of the first gramicidin channel before cessation of stirring and cessation of nystatin current spikes. (*C*) Left: Single-channel current trace showing a gA channel (*left arrow*) and a gM channel (*right arrow*), and no heterodimers. Right: A single-channel current histogram from the complete experiment shows conductance peaks at 3.4 pA (gA homodimer) and 0.9 pA (gM homodimer), with only a few heterodimers (*arrows*). PO lipids were used for the bilayer (7:3 in *n*-decane) and vesicles (2:1:1:1). $V_m = -200$ mV. Current signs are inverted.

If, indeed, the dimers do not dissociate but are internally gated, the total membrane current, $I = i^*NP_o$, should rise with increased dimer density in the liposomes and should be stationary after vesicle deposition is terminated. Therefore, the effect of increasing the peptide density in the vesicles by factors of 10 and 100 was tested. Because the heightened channel activity prevented observation of nystatin spikes, deposition was taken to end with termination of stirring based on the evidence from the single-channel studies, and was assumed to involve the fusion of approximately three to five vesicles, as was observed at the lower peptide density. The membrane currents were stationary after deposition was ended. Fig. 2 shows, for each experiment, the mean current as a function of vesicle gA density on a log-log scale. A linear increase, which is expected if the peptide molecules in the vesicles are essentially all dimerized (14), is indicated by the bottom line, an eye-guide with a slope of 1.0. A quadratic increase, which is expected if the peptide molecules are in a monomer-dominated monomer-dimer equilibrium in the vesicles (14), is indicated by the top line, an eye-guide with a slope of 2.0. The left-hand set of points derives from a subset (19) of the single-channel experiments described above. The middle and right-hand points are from the 10× and 100× density experiments. The results varied highly from experiment to experiment (perhaps related to variance in the deposition process), but display an approximate slope intermediate between 1.0 and 2.0.

The peptide density in the membranes of the vesicles used for the single-channel studies can be estimated based on the membrane area occupied per gramicidin dimer (35),

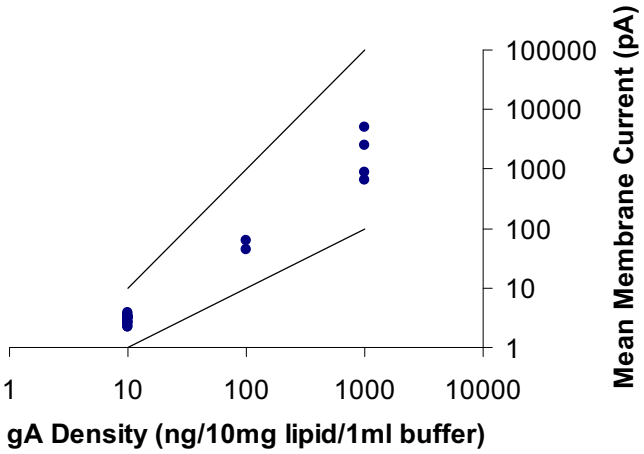

FIGURE 2 Mean membrane current during the ~30 min after the vesicle diffusion period, plotted against gA density in the vesicles. The left-hand points are the overlapping results of 20 experiments done with brain 2:1:1:1 vesicles and referred to in connection with Fig. 1, which had maximal stacking of one to eight channels. The middle and right-hand points were done with brain 7:3 vesicles and each represents the result of one experiment. In all cases, bilayers were painted with brain 7:3/decane. The lines represent a linear increase (*lower*) and a quadratic increase (*upper*), the two possible extremes expected for a monomer-dimer equilibrium in the vesicles, depending on the vesicle size and the equilibrium constant (15). Room temperature, $V_m = -200$ mV. Current signs are inverted.

~250 Å^2, and the area per lipid molecule, which we took for our mixed lipid system to be ~60 Å^2. At the lowest ratio of 10 ng gA/10 mg lipid, the nominal gA density is one peptide molecule per 0.32 μm^2 of bilayer, which corresponds to 0.4 peptide molecules per 200 nm (diameter) vesicle. Thus, one might expect three to five 200-nm vesicles to deposit only one to two gA molecules. Considering that the deposition generally yielded somewhat more (i.e., one to eight dimeric channels) in the bilayer (Fig. 1 *A* and left-hand points in Fig. 2), it is likely that vesicles that are larger in diameter or have higher peptide densities (e.g., as a statistical fluctuation) may be more prone to produce the fusion events. We proceed on the assumption that somewhat larger vesicles are the primary depositors.

The monomer [M] and dimer [D] surface densities can be predicted using the dimerization constant, K, the total gA surface density used in the liposomes, $[gA]_T$, and the equilibrium and conservation of matter equations:

$$K = \frac{[D]}{[M]^2} \tag{1}$$

$$[gA]_T = 2[D] + [M] \tag{2}$$

$$[M] = \frac{-1 + \sqrt{1 - 8K[gA]_T}}{4K} \tag{3}$$

Based on a previous measurement for a fluorescent (dansylated) gA analog in dioleoylphosphatidylcholine/decane bilayers (14), $K = 2 \times 10^{13}$ cm^2/mol, the fraction of peptide molecules participating in dimers at equilibrium (i.e., before vesicle fusion) is predicted to be 2%, 15%, and 51% for total peptide densities of 10, 100, and 1000 ng gA/10 mg lipid, respectively. On the assumptions that dansylated gA has a dimerization constant similar to that of gA, and the quantity of liposome membrane fused was the same in all of the experiments, the predicted log-log slope over the 100-fold peptide density range is 1.7, which is reasonably consistent with the observed data in Fig. 2.

NMR results

As indicated in the structural refinement based on ssNMR observations from uniformly aligned samples (9), the C=O bond of the Val_1 residue exhibits two possible orientations: one slightly toward the channel axis, and one slightly away from the channel axis. High-resolution ^{13}C MAS ssNMR (8) (Fig. 3) displays two resonances for $^{13}C_1$-labeled Val_1 gA in unoriented hydrated DMPC bilayers, indicating that the carbonyl carbon of the Val_1 residue has two different chemical environments. Both of these resonances represent carbonyls hydrogen-bonded with the Ala_5 amide across the monomer-monomer junction (8). The implication of these MAS and aligned sample results is that the carbonyl oxygen may be in two significantly different electronic environments: one in which the oxygen is in a more hydrophilic

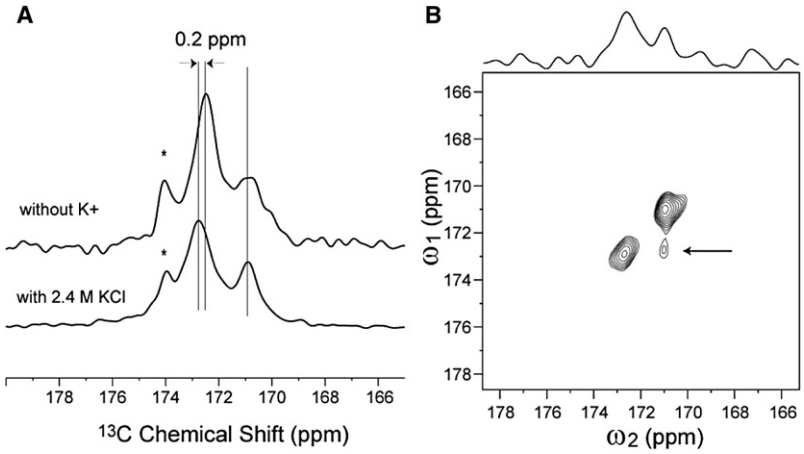

FIGURE 3 (*A*) ^{13}C MAS spectra of $^{13}C_1$-Val$_1$, ^{15}N-Ala$_5$ gA in unoriented hydrated DMPC bilayers with and without KCl in the water. Asterisks indicate the ^{13}C signals of carbonyl carbons from lipids. (*B*) 2D ^{13}C MAS chemical exchange spectrum of $^{13}C_1$-Val$_1$, ^{15}N-Ala$_5$ gA in unoriented hydrated DMPC bilayers with a mixing time of 12 s; ω_1 and ω_2 represent ^{13}C chemical shifts in the indirect and direct (or observation) dimensions, respectively, of the 2D spectrum. Above the contour plot is the spectrum taken along the direction of the arrow.

region, such as the hydrated pore interior, and one in which the carbonyl oxygen is in a more hydrophobic region, oriented toward the lipid environment. Fig. 3 *A* shows the ^{13}C MAS spectra of $^{13}C_1$-Val$_1$, ^{15}N-Ala$_5$ gA in unoriented hydrated DMPC bilayers with and without 2.4 M KCl. One of the $^{13}C_1$-Val$_1$ states (172.8 ppm) is slightly influenced (~0.2 ppm) by the presence of K^+ cations, whereas the other one (171.0 ppm) remains unchanged. This frequency shift is small but significant, especially in light of the relatively small fraction of time in which the ions reside at the center of the channel (1,36–38). Previously, shifts of $^{13}C_1$ resonances to higher parts-per-million values have been shown to be associated with ion binding (39). The relative amplitudes of the two resonance peaks suggest that the K^+-independent resonance at 171.0 ppm, which we associate with the electrically closed state, has a lower probability. This is to be expected, even though our electrophysiology experiments show the open state to have the lower probability, because 1), it is likely that either one of the two Val$_1$ gates (or the two formyl carbonyl gates) could close the channel; and 2), P_o is expected to be increased in short-chain lipids (11) like DMPC.

Fig. 3 *B* shows the 2D ^{13}C MAS chemical exchange spectrum of the same sample under the same sample conditions recorded with a mixing time of 12 s. The pulse protocol effectively allows magnetic labeling of a conformational population at the beginning of the mixing time (which, because of a long T_1 relaxation, persists for many seconds) and detection of that group's conformational distribution at the end (31). The two diagonal peaks represent the two conformational states of the $^{13}C_1$-Val$_1$, and the cross peak between them implies that the two conformational states undergo partial exchange on the mixing timescale (i.e., seconds). This is consistent with the timescale of channel gating observed electrophysiologically.

The above results demonstrate that the $^{13}C_1$-Val$_1$ carbonyl displays two chemical shifts. Two ^{13}C isotropic resonances at 164.0 and 160.8 ppm are also observed from the $^{13}C_1$-formyl gA in unoriented hydrated DMPC bilayers (with a molar peptide/lipid ratio of 1:8), as shown in Fig. 4. This implies that the carbonyl carbon of the formyl group next to the Val$_1$ residue also experiences two different chemical shift environments.

DISCUSSION

The vesicle-fusion electrophysiology results demonstrate that dimeric channels persist after converting to the closed state. These results are consistent with the high (~43.4 kT) net free-energy barrier to gA dimer in vacuo dissociation computed using normal modes tracking (40), and the observation of fluorescent resonance energy transfer from single gA dimers after termination of channel conductance (41).

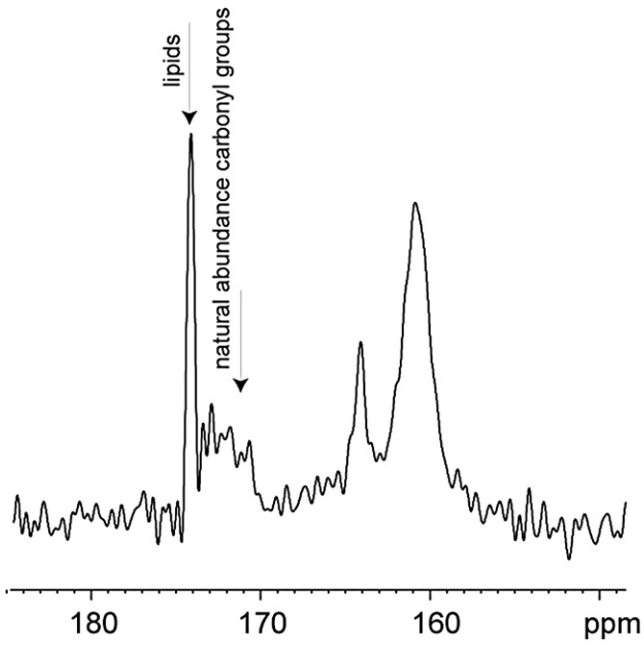

FIGURE 4 ^{13}C CPMAS NMR spectrum of $^{13}C_1$-Formyl gA in unoriented hydrated DMPC bilayers (with a molar peptide/lipid ratio of 1:8) recorded at 320 K.

Note that the computed in vacuo free-energy barrier to dissociation would be reduced by the lipid interior of dielectric 2.0 and intrachannel water molecules, but would nevertheless be expected to be very high.

The concept that channel appearance and, more particularly, channel termination reflect dimerization and monomerization has been used to interpret the effects of membrane thickness (42), peptide mutation (43), interfacial reagents (25,44), and lipid headgroup structure (45) on channel kinetics. We do not dispute the effects of these factors on channel gating, or the role of the monomer-dimer equilibrium in establishing relative homo- and heterodimer frequencies. However, the electrophysiology results reported here confirm the notion of dimer persistence through open-closed channel cycles (17) and call for a different model for the mechanism of gA channel gating. Single-dimer fluorescence colocalization in small patch pipette bilayers was suggested to occur by corralling of monomers in small rafts, bigeminate recombination, or partial dimer dissociation (17). The electrophysiological results reported here were obtained with mixed brain lipids. In such lipids, raft formation (if any) would be complex, with small domains of variable size and composition, and hard to predict. The large diameter of the bilayers used here (200 μm) would lead to a negligibly low rate of recombination of separated monomers. Local dimpling of the lipid produced by the dimer would be expected to dissipate very rapidly upon monomerization and would be unlikely to preserve colocalization. Partial disruption of hydrogen bonds at the dimer junction would leave only a small energy barrier to complete disruption (40).

We propose instead that the closed state represents a conformational variant of the intact dimer. We suggest that changes in the formyl and Val_1 carbonyl orientations (Fig. 5) represent an internal conductance gating mechanism of the dimeric ion channel that does not require the formation and dissociation of dimers. The carbonyl oxygens may facilitate conductance when they are oriented in, toward the pore, and inhibit conductance when they are oriented away from the pore.

As potential mechanisms for intact dimer channel closure, one might consider steric or energetic blockage produced by occlusion of the lumen by the N-terminal formyl residue, or complexation of a cation by multiple N-terminal carbonyl groups. The first model would require a more substantial conformational change than is described by the high-resolution structural restraints (9), and the latter mechanism would shift the isotropic and anisotropic carbonyl resonance much more substantially (39,46,47). Rather, the data here suggest that channel closure occurs by an outward libration of peptide carbonyls generating an unfavorable electrostatic environment for cations and a much increased energy barrier, effectively closing the channel without disrupting the dimer.

The ssNMR spectrum was repeated several times and the double peak was highly reproducible. The impact of ion addition in the ssNMR experiment, an 0.2 ppm shift, is small

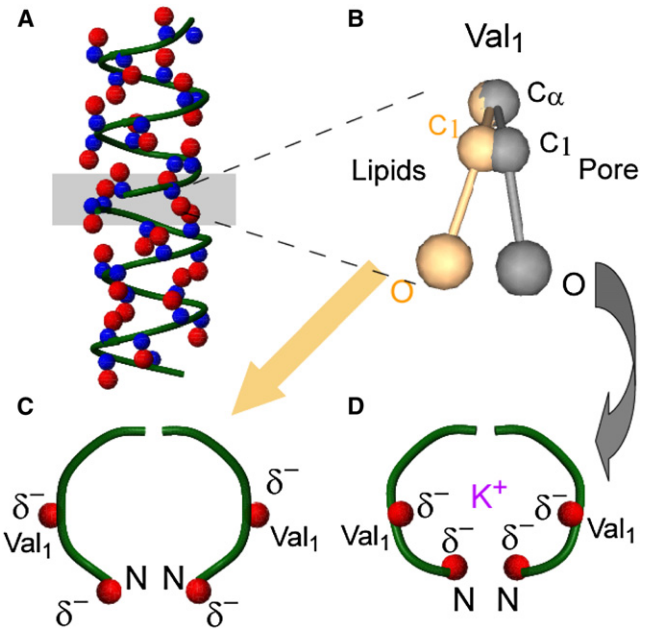

FIGURE 5 Model of the gA gating mechanism. (*A*) Backbone of the gA dimer structure from the PDB (#1MAG) showing carbonyl carbons (*blue*) and oxygens (*red*). (*B*) Side view of the Val_1 peptide plane showing two orientations of the C=O bond (one away from the pore and one toward the pore). (*C*) Top view of the monomer-monomer junction, as indicated by the gray region in *A*, showing the formyl and Val_1 oxygens oriented away from the pore. The distant location of these partial negative charges lead to a relative energetic barrier that inhibits conductance of cations. (*D*) Top view of the monomer-monomer junction, as indicated by the gray region in *A*, showing the formyl and Val_1 oxygens oriented toward the pore. The proximity of the partial negative charges of these oxygens in the channel facilitates conductance of cations.

compared to the linewidth (~1.3 ppm), but is clearly visible in the spectrum. This small shift is significant and reasonable (48), especially in light of the relatively small fraction of time in which the ions reside at the center of the channel.

The two ^{13}C resonances have the same dephasing behavior upon irradiation on the ^{15}N-labeled Ala_5 site of gA in distance measurement experiments, as was previously pointed out (8). This implies that the distance between the Val_1 carbonyl ^{13}C and the Ala_5 amide ^{15}N of the opposite monomer is essentially the same for both Val_1 conformations.

The ssNMR results reported here were obtained under conditions similar (but not identical) to those used for the electrophysiology experiments. For ssNMR, the membrane is thinner (~25 Å for the pure DMPC bilayer, as opposed to ~45 Å for the decane-inflated brain or PO phospholipid bilayers), but the higher compressibility of the solvent-inflated bilayer probably moderates the impact on gating (see below). The protein is more densely packed (1:8 gA/DMPC molar ratio in the NMR measurements, as opposed to almost infinitely dilute in the bilayer experiment), but the ssNMR structure is unchanged with reductions in density by factors of ≥ 6 (T. A. Cross, unpublished results). No

membrane potential was applied in the ssNMR studies (whereas the membrane potential was −140 mV in the bilayer experiment), but there are no formally charged atoms in gA that would be predictably perturbed by the membrane potential. These and other minor differences might have modest quantitative effects on channel conformation and function, but are not expected to have qualitative effects. The ssNMR-detected timescale of conformational change is quite approximate, so from the currently available evidence we are limited to the inference that the conformational switching timescale and distribution as detected by ssNMR have orders of magnitude similar to those observed with the planar bilayer. In conclusion, the presence of two NMR peaks with very slow interchange is reasonably consistent with the electrophysiological finding of transitions between open and closed states on a timescale of seconds.

We speculate that the changes in average open and closed times seen with changes in membrane thickness, etc., may reflect changes in the strain on the dimer junction affecting the stability of these carbonyl conformational populations. Hydrophobic mismatch was previously invoked to explain how strain on the dimer junction might disconnect the hydrogen bonds holding the monomers together (11,42). Here, we suggest that the same strain affects the conformational equilibrium between the open and closed states instead. This is good news for studies of membrane mechanical properties on gramicidin channel kinetics because, provided the number of dimers in the membrane can be ascertained accurately, it allows one to interpret the meaning of modulation of the closed and open times on the same basis. It is interesting that the gA dimers in this study remain intact in decane-inflated phospholipid bilayers. Considering the importance of hydrophobic matching in applying forces to transmembrane helices, one might expect dimers to be even more stable in thinner membranes (17), and to monomerize readily in thicker bilayers, particularly when the lipid bending modulus is high, such as in solvent-free membranes based on long-tailed lipids (18). Here, however, the painted bilayers permit dimer persistence in spite of their thickness, presumably because of the low modulus of compression for the solvent-inflated bilayer (49,50).

For years, the gA conductance mechanism was thought to be irrelevant for understanding conductance of the larger proteinaceous channels, but when the structure of KcsA was elucidated by MacKinnon and co-workers (51), it was recognized that both gA and KcsA pores were lined with peptide backbone carbonyl oxygens. As a result, numerous insights into ion permeation, including cation binding, dehydration, and selectivity, have been gleaned from studies of gA (1–5). The primary gA gating mechanism is not associated with the unique dimerization property of gA; rather, it appears to be associated with a much more general property of ion channels: local conformational changes (52). This study opens the door for examination of environmental effects on gramicidin channel gating kinetics (referenced above), as well as other ion channels (53–55), using vesicle deposition to assess oligomer behavior coupled with NMR assessment of conformer populations and dynamics.

We thank Jun Hu for preparing the NMR samples containing K^+ ions, Myriam Cotten for confirmatory NMR observations of two ^{13}C resonances, and Dixon Woodbury for help with the nystatin spike assay. We also thank Rustin Rawlings, Ben Wilson, Weston Caywood, Peter Langford, Ben Eckstrom, Nathan Green, and Luke Henderson for technical assistance, and Olaf S. Andersen, Roger E. Koeppe II, Jens Lundbaek, Peter Jordan, Genady Miloshevski, Andrew Woolley, and H. Peter Lu for helpful discussions.

The NMR spectroscopy was performed at the National High Magnetic Field Laboratory supported by the National Science Foundation (Cooperative Agreement DMR-0654118) and the State of Florida. This work was supported by a grant from the National Institutes of Health (R01 AI23007).

REFERENCES

1. Tian, F., and T. A. Cross. 1999. Cation transport: an example of structural based selectivity. *J. Mol. Biol.* 285:1993–2003.
2. Roux, B., T. Allen, …, W. Im. 2004. Theoretical and computational models of biological ion channels. *Q. Rev. Biophys.* 37:15–103.
3. Allen, T. W., O. S. Andersen, and B. Roux. 2006. Molecular dynamics—potential of mean force calculations as a tool for understanding ion permeation and selectivity in narrow channels. *Biophys. Chem.* 124:251–267.
4. Andersen, O. S., R. E. Koeppe, 2nd, and B. Roux. 2005. Gramicidin channels. *IEEE Trans. Nanobioscience.* 4:10–20.
5. Roux, B. 1996. Valence selectivity of the gramicidin channel: a molecular dynamics free energy perturbation study. *Biophys. J.* 71:3177–3185.
6. Andersen, O. S., H. J. Apell, …, A. Woolley. 1999. Gramicidin channel controversy—the structure in a lipid environment. *Nat. Struct. Biol.* 6:609–611, discussion 611–612.
7. Cross, T. A., A. Arseniev, …, B. A. Wallace. 1999. Gramicidin channel controversy—revisited. *Nat. Struct. Biol.* 6:610–611, discussion 611–612.
8. Fu, R., M. Cotten, and T. A. Cross. 2000. Inter- and intramolecular distance measurements by solid-state MAS NMR: determination of gramicidin A channel dimer structure in hydrated phospholipid bilayers. *J. Biomol. NMR.* 16:261–268.
9. Ketchem, R. R., B. Roux, and T. A. Cross. 1997. High-resolution polypeptide structure in a lamellar phase lipid environment from solid state NMR derived orientational constraints. *Structure.* 5:1655–1669.
10. Andersen, O. S., and R. E. Koeppe, 2nd. 2007. Bilayer thickness and membrane protein function: an energetic perspective. *Annu. Rev. Biophys. Biomol. Struct.* 36:107–130.
11. Hladky, S. B., and D. A. Haydon. 1972. Ion transfer across lipid membranes in the presence of gramicidin A. I. Studies of the unit conductance channel. *Biochim. Biophys. Acta.* 274:294–312.
12. Urry, D. W., M. C. Goodall, …, D. F. Mayers. 1971. The gramicidin A transmembrane channel: characteristics of head-to-head dimerized (L,D) helices. *Proc. Natl. Acad. Sci. USA.* 68:1907–1911.
13. Bamberg, E., and K. Janko. 1977. The action of a carbonsuboxide dimerized gramicidin A on lipid bilayer membranes. *Biochim. Biophys. Acta.* 465:486–499.
14. Veatch, W. R., R. Mathies, …, L. Stryer. 1975. Simultaneous fluorescence and conductance studies of planar bilayer membranes containing a highly active and fluorescent analog of gramicidin A. *J. Mol. Biol.* 99:75–92.
15. Veatch, W., and L. Stryer. 1977. The dimeric nature of the gramicidin A transmembrane channel: conductance and fluorescence energy transfer studies of hybrid channels. *J. Mol. Biol.* 113:89–102.

16. Borisenko, V., T. Lougheed, …, G. J. Schütz. 2003. Simultaneous optical and electrical recording of single gramicidin channels. *Biophys. J.* 84:612–622.

17. Harms, G. S., G. Orr, …, H. P. Lu. 2003. Probing conformational changes of gramicidin ion channels by single-molecule patch-clamp fluorescence microscopy. *Biophys. J.* 85:1826–1838.

18. Mo, Y., T. A. Cross, and W. Nerdal. 2004. Structural restraints and heterogeneous orientation of the gramicidin A channel closed state in lipid bilayers. *Biophys. J.* 86:2837–2845.

19. He, K., S. J. Ludtke, …, R. E. Koeppe, 2nd. 1994. Closed state of gramicidin channel detected by X-ray in-plane scattering. *Biophys. Chem.* 49:83–89.

20. Allen, L. C. 1975. A model for the hydrogen bond. *Proc. Natl. Acad. Sci. USA.* 72:4701–4705.

21. Honig, B. H., W. L. Hubbell, and R. F. Flewelling. 1986. Electrostatic interactions in membranes and proteins. *Annu. Rev. Biophys. Biophys. Chem.* 15:163–193.

22. Popot, J.-L., and D. M. Engelman. 1990. Membrane protein folding and oligomerization: the two-stage model. *Biochemistry.* 29:4031–4037.

23. White, S. H., and W. C. Wimley. 1999. Membrane protein folding and stability: physical principles. *Annu. Rev. Biophys. Biomol. Struct.* 28:319–365.

24. Woodbury, D. J. 1999. Nystatin/ergosterol method for reconstituting ion channels into planar lipid bilayers. *Methods Enzymol.* 294:319–339.

25. Andersen, O. S., M. J. Bruno, …, R. E. Koeppe, 2nd. 2007. Single-molecule methods for monitoring changes in bilayer elastic properties. *Methods Mol. Biol.* 400:543–570.

26. Ader, C., R. Schneider, …, M. Baldus. 2008. A structural link between inactivation and block of a K+ channel. *Nat. Struct. Mol. Biol.* 15: 605–612.

27. Huth, T., J. Schmidtmayer, …, U.-P. Hansen. 2008. Four-mode gating model of fast inactivation of sodium channel Nav1.2a. *J. Physiol.* 457:103–119.

28. Fields, C. G., G. B. Fields, …, T. A. Cross. 1989. Solid phase peptide synthesis of 15N-gramicidins A, B, and C and high performance liquid chromatographic purification. *Int. J. Pept. Protein Res.* 33:298–303.

29. Fields, G. B., C. G. Fields, …, T. A. Cross. 1988. Solid-phase peptide synthesis and solid-state NMR spectroscopy of [Ala_3-^{15}N][Val_1]gramicidin A. *Proc. Natl. Acad. Sci. USA.* 85:1384–1388.

30. Jing, N., K. U. Prasad, and D. W. Urry. 1995. The determination of binding constants of micellar-packaged gramicidin A by ^{13}C-and ^{23}Na-NMR. *Biochim. Biophys. Acta.* 1238:1–11.

31. Ernst, R. R., G. Bodenhausen, and A. Wokaun. 1987. Principles of Nuclear Magnetic Resonance in One and Two Dimensions. Clarendon Press, Oxford.

32. Helrich, C. S., J. A. Schmucker, and D. J. Woodbury. 2006. Evidence that nystatin channels form at the boundaries, not the interiors of lipid domains. *Biophys. J.* 91:1116–1127.

33. Colquhoun, D., and A. G. Hawkes. 1990. Stochastic properties of ion channel openings and bursts in a membrane patch that contains two channels: evidence concerning the number of channels present when a record containing only single openings is observed. *Proc. R. Soc. Lond. B Biol. Sci.* 240:453–477.

34. Durkin, J. T., R. E. Koeppe, 2nd, and O. S. Andersen. 1990. Energetics of gramicidin hybrid channel formation as a test for structural equivalence. Side-chain substitutions in the native sequence. *J. Mol. Biol.* 211:221–234.

35. Woolf, T. B., and B. Roux. 1996. Structure, energetics, and dynamics of lipid-protein interactions: a molecular dynamics study of the gramicidin A channel in a DMPC bilayer. *Proteins.* 24:92–114.

36. Cotten, M., C. Tian, …, T. A. Cross. 1999. Modulating dipoles for structure-function correlations in the gramicidin A channel. *Biochemistry.* 38:9185–9197.

37. Duffin, R. L., M. P. Garrett, …, D. D. Busath. 2003. Modulation of lipid bilayer interfacial dipole potential by phloretin, RH421, and 6-ketocholestanol as probed by gramicidin channel conductance. *Langmuir.* 19:1439–1442.

38. Durrant, J. D., D. Caywood, and D. D. Busath. 2006. Tryptophan contributions to the empirical free-energy profile in gramicidin A/M heterodimer channels. *Biophys. J.* 91:3230–3241.

39. Urry, D. W., K. U. Prasad, and T. L. Trapane. 1982. Location of monovalent cation binding sites in the gramicidin channel. *Proc. Natl. Acad. Sci. USA.* 79:390–394.

40. Miloshevsky, G. V., and P. C. Jordan. 2006. The open state gating mechanism of gramicidin a requires relative opposed monomer rotation and simultaneous lateral displacement. *Structure.* 14:1241–1249.

41. Lu, H. P. 2005. Probing single-molecule protein conformational dynamics. *Acc. Chem. Res.* 38:557–565.

42. Lundbaek, J. A., and O. S. Andersen. 1999. Spring constants for channel-induced lipid bilayer deformations. Estimates using gramicidin channels. *Biophys. J.* 76:889–895.

43. Becker, M. D., D. V. Greathouse, …, O. S. Andersen. 1991. Amino acid sequence modulation of gramicidin channel function: effects of tryptophan-to-phenylalanine substitutions on the single-channel conductance and duration. *Biochemistry.* 30:8830–8839.

44. Lundbaek, J. A., and O. S. Andersen. 1994. Lysophospholipids modulate channel function by altering the mechanical properties of lipid bilayers. *J. Gen. Physiol.* 104:645–673.

45. Rostovtseva, T. K., H. I. Petrache, …, S. M. Bezrukov. 2008. Interfacial polar interactions affect gramicidin channel kinetics. *Biophys. J.* 94:L23–L25.

46. Tian, F., K.-C. Lee, …, T. A. Cross. 1996. Monovalent cation transport: lack of structural deformation upon cation binding. *Biochemistry.* 35:11959–11966.

47. Hu, J., E. Y. Chekmenev, …, T. A. Cross. 2005. Ion solvation by channel carbonyls characterized by 17O solid-state NMR at 21 T. *J. Am. Chem. Soc.* 127:11922–11923.

48. Urry, D. W., J. T. Walker, and T. L. Trapane. 1982. Ion interactions in (1-13C)D-Val8 and D-Leu14 analogs of gramicidin A, the helix sense of the channel and location of ion binding sites. *J. Membr. Biol.* 69:225–231.

49. Rudnev, V. S., L. N. Ermishkin, …, Rovin YuG. 1981. The dependence of the conductance and lifetime of gramicidin channels on the thickness and tension of lipid bilayers. *Biochim. Biophys. Acta.* 642:196–202.

50. Helfrich, P., and E. Jakobsson. 1990. Calculation of deformation energies and conformations in lipid membranes containing gramicidin channels. *Biophys. J.* 57:1075–1084.

51. Doyle, D. A., J. Morais Cabral, …, R. MacKinnon. 1998. The structure of the potassium channel: molecular basis of K+ conduction and selectivity. *Science.* 280:69–77.

52. Bernèche, S., and B. Roux. 2005. A gate in the selectivity filter of potassium channels. *Structure.* 13:591–600.

53. Luchian, T., and L. Mereuta. 2006. Phlorizin- and 6-ketocholestanol-mediated antagonistic modulation of alamethicin activity in phospholipid planar membranes. *Langmuir.* 22:8452–8457.

54. Lundbaek, J. A., P. Birn, …, O. S. Andersen. 2005. Capsaicin regulates voltage-dependent sodium channels by altering lipid bilayer elasticity. *Mol. Pharmacol.* 68:680–689.

55. Perozo, E., A. Kloda, …, B. Martinac. 2002. Physical principles underlying the transduction of bilayer deformation forces during mechanosensitive channel gating. *Nat. Struct. Biol.* 9:696–703.